van der Waals Complexes between Carbonyl Fluoride and Boron Trifluoride Observed in Liquefied Argon, Krypton, and Nitrogen: A FTIR and *ab Initio* Study

A. A. Stolov,† W. A. Herrebout, and B. J. van der Veken*

Contribution from the Department of Chemistry, Universitair Centrum Antwerpen, Groenenborgerlaan 171, B2020 Antwerp, Belgium

Received March 16, 1998

Abstract: The IR spectra (4000-400 cm^{-1}) of COF_2/BF_3 mixtures, dissolved in liquefied argon (LAr), krypton (LKr), and nitrogen (LN_2), have been examined. In all spectra evidence was found for the formation of a 1:1 van der Waals complex. Using spectra recorded at several temperatures between 81 and 172 K the complexation enthalpies $\Delta H°$ in LAr, LKr, and LN_2 were determined to be −11.8(3), −10.6(3), and −7.8(3) kJ mol^{-1}, respectively. A theoretical study, using both density functional theory at the B3LYP/6-311++G(d,p) level and *ab initio* at the MP2/aug-cc-pVTZ level, indicates that the complexation can occur either via the oxygen or via a fluorine atom of COF_2. From a comparison of the experimental and calculated frequencies it was concluded that the observed complex bands are due to a species in which the boron atom coordinates with the oxygen lone pairs. The complexation energy $\Delta_c E$ is obtained from the $\Delta H°$ by correcting for solvent influences, and thermal contributions equals −15.0(6) kJ mol^{-1}. This value agrees well with the MP2/aug-cc-pVTZ level result, −12.4 kJ mol^{-1}. The complexation entropy $\Delta S°$ has been found to be influenced by the solvent and is correlated with $\Delta H°$. This correlation reflects the existence of the compensation effect for the thermodynamics of van der Waals complexes.

Introduction

Donor−acceptor complexes between Lewis acids and bases play a determining role in many catalytic processes, including Diels−Alder reactions,[1] aldol condensations,[2] and photochemical reactions.[3] As a consequence, the properties of such complexes have been the subject of extensive research, incorporating both experimental and theoretical methods. Systems, which have received considerable attention in this regard, are the complexes formed between carbonyl containing compounds and various Lewis acids.[4−17] The attention in the above research was mainly focused on the adducts with typical aldehydes such as formaldehyde, acetaldehyde, and acetone.[4−17] Much less is known about complexes formed with other carbonyl compounds such as the carbonoxohalides COF_2, COFCl, and $COCl_2$.

In the present paper we report the data on complexation of carbonyl fluoride, COF_2, with boron trifluoride, BF_3. Intermolecular interactions involving carbonyl fluoride are of interest since this compound is believed to be one of the intermediates in the photodecomposition of chlorofluorocarbons in the stratosphere.[18,19] Another motivation of the study is that COF_2 is often observed in matrix-isolation infrared experiments as a product of photolysis of various fluorine-containing compounds.[20−23] Since the formation of COF_2 is sometimes accompanied by its complexation,[21,22] knowledge of structures and energies of plausible complexes is important for interpreting the observed spectra. In addition, it may be noted that COF_2 is one of the simplest asymmetric top molecules which has been widely used for testing various theoretical models of vibrational spectroscopy.[24−28] It appears interesting to correlate the com-

* Corresponding author: bvdveken@ruca.ua.ac.be.
† Permanent address: Department of Chemistry, Kazan State University, Kremlevskaya st. 18, Kazan 420008, Russia.

(1) Honeychuck, R. V.; Hersh, W. H. *J. Am. Chem. Soc.* **1989**, *111*, 6070.
(2) Yamamoto, Y. *Acc. Chem. Res.* **1987**, *20*, 243.
(3) Lewis, F. D.; Barancyck, S. V. *J. Am. Chem. Soc*. **1989**, *111*, 8653.
(4) Shchepkin, D. N. In *Spectroscopy of Interacting Molecules*; Leningrad State University: Leningrad, 1970; p 98.
(5) LePage, T. J.; Wiberg, K. B. *J. Am. Chem. Soc.* **1988**, *110*, 6642.
(6) Muradov, G.; Tokhadze, K. G.; Atakhodzhaev, A. K. *Dokl. Akad. Nauk USSR* **1988**, 36.
(7) Branchadell, V.; Oliva A. *J. Am. Chem. Soc.* **1991**, *113*, 4132.
(8) Branchadell, V.; Sbai, A.; Oliva A. *J. Phys. Chem.* **1995**, *99*, 6472.
(9) Legon, A. C. *J. Chem. Soc., Faraday Trans.* **1996**, *92*, 2677.
(10) Jasien, P. G. *J. Phys. Chem.* **1992**, *96*, 9273.
(11) Schriver, L.; Abdelaoui, O.; Schriver, A. *J. Phys. Chem.* **1992**, *96*, 8069.
(12) Abdelaoui, O.; Schriver, L.; Schriver, A., *J. Mol. Struct*. **1992**, *268*, 335.
(13) Coxon, J. M.; Luibrand, R. T. *Tetrahedron Lett.* **1993**, *44*, 7093.
(14) Nowek, A.; Leszczynski, J. *J. Chem. Phys.* **1996**, *104*, 1441.
(15) Dudis, D. S.; Everhart, J. B.; Branch, T. M.; Hunnicutt, S. S. *J. Phys. Chem.* **1996**, *100*, 2083.
(16) Ammal, S. S. C.; Venuvanalingam, P. *J. Chem. Phys.*, **1997**, *107*, 4329.
(17) Kang, H. C. *J. Mol. Struct. (Theochem)* **1997**, *401*, 127.
(18) Duxbury, G.; McPhail, M. L. W.; McPheat, R. *J. Mol. Spectr.* **1997**, *182*, 118.
(19) Duxbury, G.; McPhail, M. L. W.; McPheat, R. *J. Chem. Soc., Faraday Trans.* **1997**, *93*, 2731.
(20) Milligan, D. E.; Jacox, M. E.; Bass, A. M.; Comeford, J. J.; Mann, D. E. *J. Chem. Phys.* **1965**, *42*, 3187.
(21) Smardzewski, R.; De Marco, R. A.; Fox, W. B. *J. Chem. Phys*. **1975**, *63*, 1083.
(22) Smardzewski, R.; Fox, W. B. *J. Phys. Chem.* **1975**, *79*, 219.
(23) David, S. J.; Ault, B. S. *Inorg. Chem.* **1985**, *24*, 1238.
(24) McKean, D. C.; Bruns, R. E.; Person, W. B.; Segal, G. A. *J. Chem. Phys.* **1971**, *55*, 2890.
(25) Mallinson, P. D.; McKean, D. C.; Holloway, J. H.; Oxton, I. A. *Spectrochim. Acta* **1975**, *31A*, 143.
(26) Bohn, R. K.; Casleton, K. H.; Rao, Y. V. C.; Flynn, G. W. *J. Phys. Chem.* **1982**, *86*, 736.
(27) Nikolova B.; Galabov, B.; Lozanova, C. *J. Chem. Phys.* **1983**, *78*, 4828.
(28) Martins, F. H. P.; Bruns, R. E. *Spectrochim. Acta* **1997**, *53A*, 2115.

S0002-7863(98)00874-9 CCC: $15.00
Published on Web 07/11/1998

plexation effect on vibrational spectra with some of the theoretical predictions.

The Lewis acid used in this study, boron trifluoride, is known to be an effective catalyst for a variety of inorganic and organic reactions.[29] Molecular complexes of the boron trihalides have been studied for many years and are well characterized in different media.[30−32] In contrast, only a few studies have been published in which COF_2 complexes were discussed. Shea and Campbell[33] have reported the formation of a weak adduct between COF_2 and Ar using molecular beams experiments. Andrews *et al*.[34] and Clemitshaw and Sodeau[35] have described the infrared spectra of complexes between carbonyl fluoride and iodomonofluoride (IF) formed in argon matrices. More recently, the complexes formed between COF_2 and chlorine were studied by Bouteiller *et al*.,[36] using matrix-isolation spectroscopy and *ab initio* calculations at the MP2/6-31+G** level. To our knowledge, no complexes formed between boron halides and carbonoxohalides have yet been reported.

Of particular interest in the COF_2/BF_3 system is the fact that COF_2 has different sites for coordination with a BF_3 molecule. In analogy with the results obtained for aldehydes,[5,7−9] BF_3 can be expected to interact with the oxygen lone pairs. However, BF_3 also forms complexes with alkyl fluorides,[37,38] so that a second type of complex may be expected, in which BF_3 binds to one of the fluorine atoms. Finally, complexes of BF_3 with π systems have been reported,[38,39] and it cannot be excluded *a priori* that a complex is formed with the π bond in COF_2.

In this study, infrared spectra have been recorded of COF_2/BF_3 mixtures dissolved in cryosolutions, using liquefied argon (LAr), krypton (LKr), and nitrogen (LN_2) as solvents. It will be shown in the following paragraphs that the formation of a complex is observed. For this complex, the stoichiometry and complexation enthalpy have been determined, and its structure has been derived from a comparison of the experimental spectra with *ab initio* predictions.

Experimental Section

Boron trifluoride and carbonyl fluoride (CP grade) were obtained from Union Carbide and Fluorochem Limited, respectively. The solvent gases Ar, Kr, and N_2 were supplied by L'Air Liquide and have a stated purity of 99.9999, 99.9999, and 99.998%, respectively. The IR spectra of liquefied krypton show the presence of a small amount of SiF_4 and CF_4, the concentrations being approximately $10^{-5}-10^{-6}$ M. A small amount of SiF_4 was also detected in the BF_3 used. The solvent gases and BF_3 were used without further purification.

The carbonyl fluoride as obtained was found to contain $COCl_2$ (≈1%) and COClF (≈0.5%). Before use, the sample was purified on a low-pressure low-temperature fractionation column.

The infrared spectra were recorded on Bruker IFS 113v and Bruker IFS 66v interferometers, using a Globar source, a Ge/KBr beamsplitter, and a broad band MCT detector. The interferograms were averaged over 200 scans, Blackman-Harris apodized and Fourier transformed using a zero filling factor of 4, to yield spectra at a resolution of 0.5 cm^{-1}.

The cryosolution setup consists of a pressure manifold needed for filling and evacuating the cell and for monitoring the amount of solute gas used in a particular experiment, and of the actual cell, machined from a massive copper block. The cell is equipped with wedged Si windows and has an optical path length of 40 mm. Details have been previously described.[40,41]

The density functional theory (DFT) calculations were carried out using Gaussian94.[42] For all calculations, Becke's three-parameter exchange functional[43] was used in combination with the Lee−Yang−Parr correlation functional,[44] while the 6-311++G(d,p) basis set was used throughout as a compromise between accuracy and applicability to larger systems. To reduce the errors arising from the numerical integration, for all calculations the *finegrid* option, corresponding to roughly 7000 grid points per atom, was used.

For the complex species more accurate values for the complexation energy were obtained using *ab initio* calculations at the MP2(=full)/aug-cc-pVTZ level.

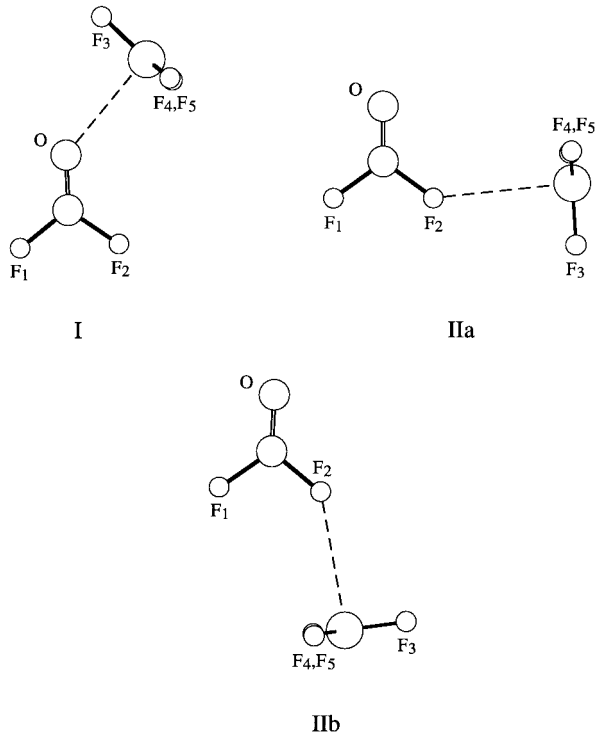

Figure 1. B3LYP/6-311++G(d,p) equilibrium geometries for the 1:1 complexes between carbonyl fluoride, COF_2, and boron trifluoride, BF_3.

Results

(A) *Ab Initio* Calculations. DFT calculations starting from several positions of COF_2 with respect to BF_3 have been made.

(29) Greenwood, N. N.; Earnshaw, A. *Chemistry of the Elements*; Pergamon: Oxford, 1984; p 220.
(30) Nxumalo, L. M.; Ford, T. A. *J. Mol. Struct. (Theochem.)* **1996**, *369*, 115 and references therein.
(31) Sluyts, E. J.; Van der Veken, B. J. *J. Am. Chem. Soc.* **1996**, *118*, 440.
(32) Van der Veken, B. J.; Sluyts, E. J. *J. Am. Chem. Soc.* **1997**, *119*, 11516.
(33) Shea, J. A.; Campbell, E. J. *J. Chem. Phys.* **1983**, *79*, 4724.
(34) Andrews, L.; Hawkins, M.; Withnall, R. *Inorg. Chem.* **1985**, *24*, 4234.
(35) Clemitshaw, K. C.; Sodeau, J. R. *J. Phys. Chem.* **1989**, *93*, 3552.
(36) Bouteiller, Y.; Abdelaoui, O.; Schriver, A.; Schriver-Mazzuoli, L. *J. Chem. Phys.* **1995**, *102*, 1731.
(37) Sluyts, E. J.; Van der Veken, B. J. *J. Phys. Chem.* **1997**, *101A*, 9070.
(38) Herrebout, W. A.; Lundell, J.; Van der Veken, B. J. Manuscript in preparation.
(39) Herrebout, W. A.; Van der Veken, B. J. *J. Am. Chem. Soc.* **1997**, *119*, 10446.
(40) Van der Veken, B. J.; De Munck, F. R. *J. Chem. Phys.* **1992**, *97*, 3060.
(41) Van der Veken, B. J. Infrared Spectroscopy in Liquefied noble gases. In *Low Temperature Molecular Spectroscopy*; Fausto, R., Ed.; Kluwer Academic Publishers: Dordrecht, 1996.
(42) Gaussian 94, Revision B2; Frisch, M. J.; Trucks, G. W.; Schlegel, H. B.; Gill, P. M. W.; Johnson, B. G.; Robb, M. A.; Cheeseman, J. R.; Keith, T.; Petersson, G. A.; Montgomery, J. A.; Raghavachari, K.; Al-Laham, M. A.; Zakrzewski, V. G.; Ortiz, J. V.; Foresman, J. B.; Cioslowski, J.; Stefanov, B. B.; Nanayakkara, A.; Challacombe, M.; Peng, C. Y.; Ayala, P. V.; Chen, W.; Wong, M. W.; Andres, J. L.; Replogle, E. S.; Gomperts, R.; Martin, R. L.; Fox, D. J.; Binkley, J. S.; Defrees, D. J.; Baker, J.; Stewart, J. P.; Head-Gordon, M.; Gonzalez, C.; and Pople, J. A. Gaussian, Inc.: Pittsburgh PA, 1995.
(43) Becke, A. D. *J. Chem. Phys.* **1993**, *98*, 5648.
(44) Lee, C.; Yang, W.; Parr, R. G. *Phys. Rev. B* **1988**, *37*, 785.

Table 1. B3LYP/6-311++G(d,p) Structural Parameters[a] for **I**, **IIa**, and **IIb**

parameter	**I**	**IIa**	**IIb**	CF_2O	BF_3
r(C═O)	1.1744	1.1696	1.1693	1.1710	
r(C−F_1)	1.3161	1.3180	1.3184	1.3219	
r(C−F_2)	1.3162	1.3290	1.3291	1.3219	
r(O···B)	2.6628				
r(F_2···B)		2.9609	2.9523		
r(B−F_3)	1.3177	1.3183	1.3173		1.3177
r(B−F_4)	1.3205	1.3178	1.3184		1.3177
r(B−F_5)	1.3205	1.3178	1.3184		1.3177
∠(O−C−F_1)	125.713	126.782	126.775	126.188	
∠(O−C−F_2)	126.048	125.845	125.780	126.188	
∠(F_1−C−F_2)	108.239	107.374	107.554	107.624	
∠(C═O···B)	136.780				
∠(O···B−F_3)	91.805				
∠(O···B−F_4)	91.052				
∠(O···B−F_5)	91.038				
∠(C−F_2···B)		137.624	138.519		
∠(F_2···B−F_3)		87.211	91.762		
∠(F_2···B−F_4)		91.692	89.359		
∠(F_2···B−F_5)		91.692	89.359		
∠(F_3−B−F_4)	120.047	119.951	120.041		120.000
∠(F_3−B−F_5)	120.048	119.951	120.041		120.000
∠(F_4−B−F_5)	119.753	120.094	119.917		120.000
τ(B···O−C−F_1)	179.96				
τ(B···O−C−F_2)	−0.05				
τ(F_3−B···O−C)	179.98				
τ(F_4−B···O−C)	59.88				
τ(F_5−B···O−C)	−59.91				
τ(B···F_2−C−O)		0.00	180.00		
τ(B···F_2−C−F_1)		180.00	0.00		
τ(F_3−B···F_2−C)		180.00	180.00		
τ(F_4−B···F_2−C)		60.09	59.96		
τ(F_5−B···F_2−C)		−60.09	−59.96		
E/Hartree	−637.784496	−637.781764	−637.781733	−313.116608	−324.664142
ΔE/kJ mol^{-1}	−9.84	−2.66	−2.58		
μ/Debye	1.54	0.89	0.76	0.94	0.00

[a] Bond length in Å, bond angles in deg.

These converge into three different isomers, which are shown in Figure 1. Their structural parameters and complexation energies, defined as the energy of the complex from which the monomer energies have been subtracted, are collected in Table 1.

In a π complex between BF_3 and COF_2, the monomers must be expected to have their planes parallel to each other. Starting calculations with this structural characteristic, however, did not converge to stable structures.

In the more stable isomer, **I**, BF_3 binds to a lone pair of the oxygen atom, while in the stable structures **IIa** and **IIb** the electron deficient B atom interacts with a fluorine atom of COF_2. For isomers **IIa** and **IIb** the boron atom is situated in the plane of COF_2. For isomer **I** the predicted energy minimum corresponds to a slightly nonsymmetric structure, with the boron atom out of the plane formed by the C, O, and F_2 atoms (Table 1). However, the deviations from C_s symmetry are very small, and it cannot be excluded that the asymmetry is an artifact of the DFT calculations. It should be noted that for isomer **I** the structure is in agreement with the rules suggested by Legon and Millen.[45] The tilt angle of the BF_3 symmetry axis with the van der Waals bond, defined in the usual way,[46] is −0.5, 3.0, and −1.6 degrees for **I**, **IIa**, and **IIb**, respectively. The valency angles between the B−F bonds and the van der Waals bond indicate that the planarity of BF_3 is slightly affected. The nonplanarity can be measured as the angle between a B−F bond and a plane perpendicular to the BF_3 symmetry axis, which is found to be 1.30, 0.20, and 0.16 degrees for **I**, **IIa**, and **IIb**, respectively. The data in Table 1 also show minor changes in the structure between monomers and complexes. These are readily understood from donor−acceptor considerations[47] and will not be discussed in detail.

The fact that three isomers have been found in the *ab initio* calculations confirms the anticipated presence of different interaction sites in COF_2. However, the two types of complexes are not equally probable: if we assume that the corrections transforming energies into free enthalpies are similar for the three complexes, the energies in Table 1 predict that at 100 K, a characteristic temperature in our experiments, the equilibrium populations of **IIa** and **IIb** are less than 0.02% that of **I**. Even if we allow for the approximations made, these low fractions suggest it is unlikely that **IIa** and **IIb** can be detected. It will be shown below that this is confirmed by the infrared spectra.

The predicted vibrational frequencies and infrared intensities for monomers and the complexation shifts for **I**, **IIa**, and **IIb**, defined as $\Delta\tilde{\nu} = \tilde{\nu}_{\text{complex}} - \tilde{\nu}_{\text{monomer}}$, are summarized in Table 2. Because of the relatively weak interaction between the monomers, the vibrations of the complexes can easily be subdivided into modes localized in the COF_2 and BF_3 moieties and into intermolecular (van der Waals) modes. The van der Waals modes are all predicted to give rise to very weak bands in the far infrared. This region was not investigated, and thus only modes localized in COF_2 and in BF_3 will be discussed here. The latter can unambiguously be correlated with the modes of the isolated monomers. Therefore, we will describe

(45) Legon, A. C. *Chem. Phys. Lett.* **1997**, *297*, 55.

(46) Pross, A.; Radom, L.; Riggs, N. V. *J. Am. Chem. Soc.* **1980**, *102*, 2253.

(47) Gutman, V. *The Donor Acceptor Approach to Molecular Interactions*; Plenum Press: New York, 1988.

Table 2. B3LYP/6-311++G(d,p) Vibrational Frequencies (cm^{-1}) and Infrared Intensities (km mol^{-1}) for COF_2, $^{10}BF_3$, and $^{10}BF_3$[c]

mode symmetry[a,b]		COF_2		BF_3				**I**		**IIa**		**IIb**	
				^{11}B		^{10}B							
		$\tilde{\nu}$	int.	$\tilde{\nu}$	int.	$\tilde{\nu}$	int.	$^{11}B\ \Delta\tilde{\nu}$	$^{10}B\ \Delta\tilde{\nu}$	$^{11}B\ \Delta\tilde{\nu}$	$^{10}B\ \Delta\tilde{\nu}$	$^{11}B\ \Delta\tilde{\nu}$	$^{10}B\ \Delta\tilde{\nu}$
$\nu_1^{COF_2}$	A_1	1973.3	520.8					−15.1	−15.1	7.4	7.4	8.8	8.8
$\nu_2^{COF_2}$	A_1	954.7	68.2					14.2	14.2	−3.5	−3.5	−3.7	−3.7
$\nu_3^{COF_2}$	A_1	575.5	5.8					3.6	3.6	0.9	0.9	−0.3	−0.3
$\nu_4^{COF_2}$	B_2	1199.9	483.5					28.8	28.9	−6.9	−6.8	−9.7	−9.6
$\nu_5^{COF_2}$	B_2	614.7	6.4					6.5	7.0	−0.3	−0.3	0.0	0.0
$\nu_6^{COF_2}$	B_1	772.1	39.4					4.0	4.0	−2.8	−2.8	−2.3	−2.3
$\nu_1^{BF_3}$	A_1'			868.8		868.8		−6.2	−6.1	−0.2	−0.9	−0.8	−1.8
$\nu_2^{BF_3}$	A_2'			681.9	102.2	709.7	110.7	−31.0	−33.0	−7.4	−7.7	−8.5	−8.9
$\nu_3^{BF_3}$	E'			1416.9	975.2	1468.9	1067.6	−2.8	−2.9	0.0	0.0	0.7	0.7
								−13.6	−14.0	−2.7	−2.8	−3.4	−3.5
$\nu_3^{BF_3}$	E'			465.7	29.6	467.5	28.8	−0.4	−0.3	0.4	0.4	0.4	0.5
								−1.2	−1.1	0.1	0.1	−0.1	−0.1

[a] The normal modes for COF_2 are denoted as follows: $\nu_1^{COF_2}$ is the C═O stretch, $\nu_2^{COF_2}$ is the CF_2 symmetric stretch, $\nu_3^{COF_2}$ is the COF_2 in plane deformation, $\nu_4^{COF_2}$ is the CF_2 asymmetric stretch, $\nu_5^{COF_2}$ is the COF_2 in-plane asymmetric deformation, $\nu_6^{COF_2}$ is the COF_2 out-of-plane deformation. [b] The normal modes of BF_3 are identified as follows: $\nu_1^{BF_3}$ is the BF_3 symmetric stretch, $\nu_2^{BF_3}$ is the BF_3 out-of-plane deformation, $\nu_3^{BF_3}$ is the BF_3 asymmetric stretch, $\nu_4^{BF_3}$ is the BF_3 asymmetric deformation. [c] Complexation shifts (cm^{-1}) for **I**, **IIa**, and **IIb**.

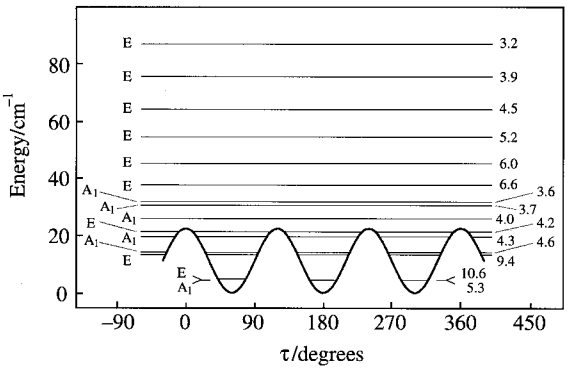

Figure 2. The potential and energy levels for the rotation of BF_3 against COF_2 in isomer **I**. The symmetry species of the levels, and their population, in %, are shown on the left and right hand sides of the figure, respectively.

them using the assignments of the monomer vibrations. For the latter, the standard numbering scheme is used, and the symbol is expanded with the formula of the monomer as a superscript. The complexation shifts of Table 2 will be discussed below, in relation to the experimental spectra.

Inherent to the weakness of the van der Waals bond is the flexibility of the complex. For isomer **I** this can be characterized by calculating (i) the barrier hindering internal rotation of the monomers around the van der Waals bond and (ii) the barrier hindering interconversion between **I** and its mirror image, in which <C═O···B equals 223.22 degrees. The barriers were obtained by systematically varying the required angular parameter, at each value of these relaxing all other structural parameters. The resulting barriers are 0.26 kJ mol^{-1} for the internal rotation and 1.02 kJ mol^{-1} for the interconversion. The calculations indicate that the two internal motions are slightly coupled: when the dihedral angle measuring the internal rotation, τ(C═O···B−F), is changed from 180° to 120°, the relaxed value of the angle that measures the interconversion, <C═O···B, changes from 137.78° to 142.11°.

The implications of the low barrier on the vibrational behavior of the complex were explored using a simplified model in which the internal rotation and the interconversion are treated as uncoupled motions. The Hamiltonian for a one-dimensional internal motion described by a coordinate τ can be written[48] in terms of the kinetic constant $B = (-\hbar^2/2)g_{44}(\tau)$ and the potential energy function $V(\tau)$. For a periodic motion like the internal rotation, B and $V(\tau)$ are developed in a Fourier series, and a free rotor base is used to set up the Hamiltonian matrix, while for the interconversion they are written in a power series, and a harmonic oscillator basis is used. To ensure convergence, in both cases 300 basis functions were used. For the internal rotation, g_{44} is only weakly dependent on τ(C═O···B−F) and was approximated to equal the constant zeroth order term, calculated to be 0.526 cm^{-1}. The potential energy was described by the simple 3-fold barrier $V(cm^{-1}) = 11.02(1 + \cos 3\tau)$. The energy levels that are significantly populated at 100 K are shown in Figure 2.

For the interconversion, the kinetic constants, calculated at a 5-degree interval, were found to be accurately fitted by the polynomial

$$B(cm^{-1}) = 0.4065 - 0.2638\varphi^2 + 0.1363\varphi^4 - 0.0305\varphi^6 \quad (1)$$

with φ equal to (π − <C═O···B). For the *ab initio* potential a satisfactory fit was obtained only by adding an exponential term to the 2/4-double minimum potential

$$V(\varphi) = A\varphi^2 + B\varphi^4 + C\exp(-D\varphi^2) + E \quad (2)$$

where $A = -295.68$ cm^{-1}, $B = 281.90$ cm^{-1}, $C = 150.30$ cm^{-1}, $D = 0.00226$, and $E = -70.00$ cm^{-1}. The resulting energy levels, their symmetry labels, and their populations at 100 K are shown in Figure 3.

It can be seen in Figure 2 that even at 100 K the largest fraction of the complex molecules is thermally excited in levels above the barrier. Thus, the composing molecules must be regarded as performing a nearly free internal rotation. The situation is less extreme in Figure 3, but nevertheless an important fraction of the molecules is populating the first few excited states, which are either very close to the barrier or above it. So, on top of the internal rotation, the complex exhibits very large amplitude deformations. From these calculations the view emerges that the complex is extremely nonrigid. This is of consequence for the vibrational spectra of the complex, as will be discussed below.

(48) Harthcock, M. A.; Laane, J. *J. Phys. Chem.* **1985**, *89*, 4231.

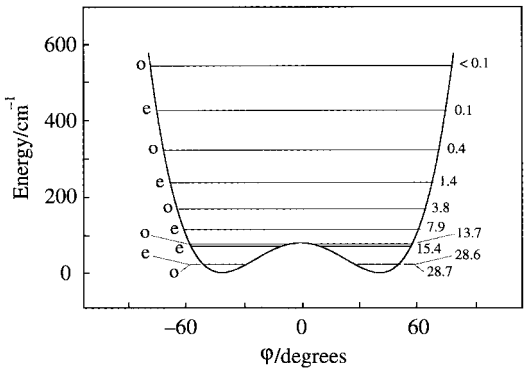

Figure 3. The double minimum potential for the large amplitude C═O···B deformation in isomer **I**. The angle φ equals (π − <C═O···B). The symmetry species of the levels, and their population, in %, are shown on the left and right hand sides of the figure, respectively.

(B) Infrared Spectra. The vibrational spectra of carbonyl fluoride in different phases, including cryosolutions in liquid argon (LAr), are well documented.[24,25,49,50] The infrared spectra obtained in this work are similar to those published by Mallinson *et al*.[25] (vapor phase) and Shchepkin *et al*.[49] (solution in liquefied argon).

The formation of COF_2 oligomers has been observed in argon matrices by Mallinson *et al*.[25] Therefore, the spectra recorded in this study were scrutinized for the presence of self-associated species. However, for none of the solvents, even at the lowest temperatures of the more concentrated solutions, were bands attributable to a new species observed, from which was concluded that the concentration of oligomers was below the detection limit.

The infrared spectrum of boron trifluoride in cryosolution has been previously described in detail[31] and need not be commented upon here.

Unless stated otherwise the spectra discussed below were measured in LAr solutions. As band maxima in cryosolutions show important temperature gradients,[31,51,52] also the temperature at which the spectrum was recorded is specified. Spectra observed in LKr and LN_2, apart from minor frequency shifts and differences in relative intensities of the complex bands, are quite similar to those in LAr and will not be discussed separately.

In LAr, the solubility of BF_3 is 2×10^{-3} M at 85 K.[31] For COF_2, at the same temperature, the solubility is found to be much lower, 1×10^{-4} M, although it rises sharply with temperature. Consequently, only solutions with relatively low concentrations of the monomers could be prepared. In spite of this, pronounced changes are observed in the spectra when mixed solutions are investigated. This is illustrated in Figure 4, in which the spectrum of a solution in LAr containing approximately 1.4×10^{-4} M COF_2 and 8.4×10^{-3} M BF_3 is compared with the spectra of a solution containing only COF_2 and that of a solution containing only BF_3. From left to right the regions of $\nu_4^{COF_2}$, $\nu_2^{COF_2}$, and $\nu_6^{COF_2}$ are shown. For each region, a new band is present in the spectrum of the mixed solution. Analogous new bands are observed near $\nu_3^{COF_2}$ and $\nu_5^{COF_2}$. Their presence proves that a complex between COF_2 and BF_3 is being formed. Frequencies of the observed bands are collected in Table 3.

In the same spectra, changes are also observed in the region of the carbonyl stretching, $\nu_1^{COF_2}$, which is given in Figure 5.

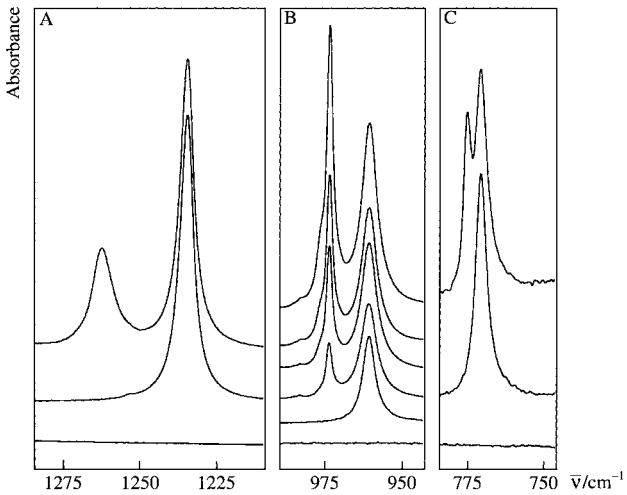

Figure 4. Details of the midinfrared spectra of COF_2/BF_3 mixtures dissolved in liquefied argon: (A) the $\nu_4^{COF_2}$ region; (B) the $\nu_2^{COF_2}$ region; (C) the $\nu_6^{COF_2}$ region. The lower two spectra were recorded from solutions containing only BF_3 and COF_2, respectively. The temperatures of the samples are 106.4 K for (A) and (C) and 115.6 K for (B). For (A) and (C) the concentrations used are 8.4×10^{-3} M for BF_3 and 1.4×10^{-4} M for COF_2. For (B) the concentration of BF_3 increases from top to bottom from 1×10^{-2} to 1×10^{-1} M.

Table 3. Experimental Frequencies (cm^{-1}) for CF_2O, BF_3, $CF_2O{\cdot}BF_3$ Complex in Liquid Argon (100 K) and the B3LYP/6-311++G(d,p) Data for the Complex-Monomer Frequency Shifts

mode	monomer bands	complex bands	$\Delta\tilde{\nu}_{exp}$	$\Delta\tilde{\nu}_{calcd}$[a] I	IIa	IIb
			CF_2O Submolecule			
$\nu_1^{COF_2}$	1937.1	1909.3	−27.8	−15.1	7.4	8.8
$\nu_2^{COF_2}$	960.3	973.2	12.9	14.2	−3.5	−3.7
$\nu_3^{COF_2}$	580.6	584.5	3.9	3.6	0.9	−0.3
$\nu_4^{COF_2}$	1234.8	1261.3	26.5	28.9	−6.9	−9.7
$\nu_5^{COF_2}$	618.5	625.4	6.6	6.5	−0.3	0.0
$\nu_6^{COF_2}$	770.2	773.9	3.7	4.0	−2.8	−2.3
$2\nu_6^{COF_2}$	1540.3	1549.0	8.7	(8.0)[c]	(−5.6)	(−4.6)
$\nu_2^{COF_2} + \nu_5^{COF_2}$	1578.1	1598.0	19.9	(20.7)	(−3.8)	(−3.7)
$2\nu_2^{COF_2}$	1907.5	1949.2	41.7	(28.2)	(−7.0)	(−7.4)
$2\nu_4^{COF_2}$	2459.6	2513.0	53.4	(57.8)	(−13.8)	(−19.4)
$2\nu_1^{COF_2}$	3829.7	3797.2	−32.5	(−30.2)	(14.8)	(17.6)
			$^{11}BF_3$ submolecule			
$\nu_1^{BF_3}$		867.0		−6.2	−0.9	−0.8
$\nu_2^{BF_3}$	680.3	650.7	−29.4	−31.0	−7.4	−8.5
$\nu_3^{BF_3}$	1444.3	1438.5	−5.8	−8.2[b]	−1.4[b]	−1.3[b]
$\nu_4^{BF_3}$	470.7			−0.8[b]	0.3[b]	0.1[b]
$\nu_1^{BF_3} + \nu_4^{BF_3}$	1358.0	1351.7	−6.3	(−7.0)	(−0.6)	(−0.9)
$\nu_1^{BF_3} + \nu_3^{BF_3}$	2325.1	2314.1	−11.0	(−14.4)	(−2.3)	(−2.3)
			$^{10}BF_3$ Submolecule			
$\nu_1^{BF_3}$		867.0		−6.1	−0.9	−1.0
$\nu_2^{BF_3}$	707.9			−33.0	−7.7	−8.9
$\nu_3^{BF_3}$	1495.6	1489.6	−6.0	−8.5[b]	−1.4[b]	−1.4[b]
$\nu_4^{BF_3}$	470.7			−0.7[b]	0.3[b]	0.2[b]
$\nu_1^{BF_3} + \nu_4^{BF_3}$	1358.0	1351.7	−6.3	(−6.8)	(−0.6)	(−0.8)
$\nu_1^{BF_3} + \nu_3^{BF_3}$	2375.3	2363.9	−11.4	(−14.6)	(−2.3)	(−2.4)

[a] The values given in brackets were estimated on the basis of the band assignment of combination modes. [b] Averaged over two nondegenerate modes.

(49) Belozerskaya, L. P.; Zhigula, L. A.; Shchepkin D. N. *Opt. Spectrosc. (USSR)* **1979**, *47*, 267.
(50) Craig, N. C. *Spectrochim. Acta* **1988**, *44A*, 1225.
(51) Bulanin, M. O. *J. Mol. Struct.* **1973**, *19*, 59.
(52) Bulanin, M. O.; Orlova, N. D.; Zelikina, G. Ya. In *Molecular Cryospectroscopy*; Clark, R. J. H., Hester, R. E., Eds.; Wiley: Chichester, 1995; p 37.

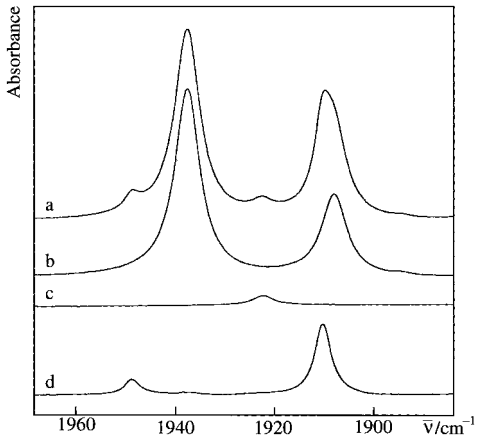

Figure 5. The $\nu_1^{COF_2}$ region of the midinfrared spectra of COF_2/BF_3 solutions in liquefied argon, at 115.7 K: (a) solution containing both BF_3 and COF_2; (b) solution containing only COF_2; (c) solution containing only BF_3; (d) spectrum of the "pure complex" obtained by rescaled subtraction of (b) and (c) from (a). The concentrations used are 8.4×10^{-3} M for BF_3 and 1.4×10^{-4} M for COF_2.

Table 4. Fermi Resonance in the $\nu_1^{COF_2} - 2\nu_2^{COF_2}$ System of Carbonyl Fluoride: Experimental and Unperturbed Frequencies (cm^{-1}) for COF_2 Monomer (ν_m) and $COF_2 \cdot BF_3$ (ν_c) in Liquefied Argon at 100 K

	experimental frequencies			unperturbed frequencies[a]		
mode	ν_m	ν_c	$\nu_c - \nu_m$	ν_m	ν_c	$\nu_c - \nu_m$
$\nu_1^{COF_2}$	1937.1	1909.3	−27.8	1928.0	1916.0	−12.0
$2\nu_2^{COF_2}$	1907.5	1949.2	41.7	1916.6	1942.7	26.1
$\nu_2^{COF_2}$	960.3	973.2	12.9			(12.9)

[a] Calculated using the Intensity method.[53−55]

For the monomer COF_2 solution, the Fermi resonance between $\nu_1^{COF_2}$ and $2\nu_2^{COF_2}$ leads to the presence of two bands of similar intensity. For the mixed solution, a new band is clearly observed only at 1949.2 cm^{-1}. The situation becomes much clearer when the monomer contributions are subtracted out, using rescaled spectra recorded at the same temperature, of solutions containing only either of the monomers. This results in spectrum 5d: it can be seen that for the mixed solution another new band is present, at 1909.3 cm^{-1}. Together with the 1949.2 cm^{-1} they form the Fermi doublet in the complex. Comparison of the spectra 5b and 5d shows that the complexation not only shifts the bands, but also inverts their relative intensity. Hence, the complexation shifts the unperturbed overtone $2\nu_2^{COF_2}$ from the low frequency side of $\nu_1^{COF_2}$ to the high frequency side. This is related to the blue shift of the fundamental $\nu_2^{COF_2}$, Figure 4b, and is also determined by the complexation shift of $\nu_1^{COF_2}$. Insight in this is obtained from unperturbed frequencies of monomer and complex, which were derived using the intensity method.[53−55] The observed intensities of $\nu_1^{COF_2}$ and $2\nu_2^{COF_2}$ needed for the analysis were determined by least squares fitting, using Gauss/Lorentz sum functions, of the region shown in Figure 5 (parts b and d). The resulting unperturbed frequencies are collected in Table 4. They have been assigned on the basis of the observed relative intensities. Thus, for the monomer, $\nu_1^{COF_2}$ is assigned to the high frequency component, and for the complex to the low frequency component. It can be seen that the unperturbed $\nu_1^{COF_2}$ shifts by -12.0 cm^{-1} upon complexation, while the unperturbed $2\nu_2^{COF_2}$ shifts by $+26$ cm^{-1}. The blue shift of the latter is very nearly twice the shifts observed for the fundamental, 12.9 cm^{-1}. This is in line with expectations.

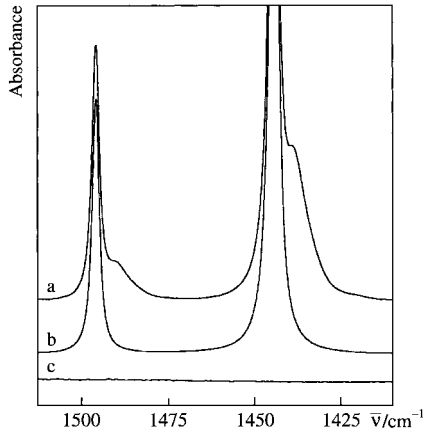

Figure 6. The $\nu_3^{BF_3}$ region of the mid-infrared spectra of solutions in liquefied argon, at 104.0 K: (a) solution containing only BF_3; (b) solution containing both BF_3 and COF_2; (c) solution containing only COF_2. The concentrations used are 3.4×10^{-4} M for BF_3 and 8.2×10^{-3} M for COF_2.

At the concentrations used to record the spectra in Figures 4 and 5, no complex bands located in BF_3 could be detected. They are observed in spectra of solutions containing larger relative amounts of COF_2, which, in view of the solubilities, had to be studied at higher temperatures. This is illustrated in Figure 6, in which the $\nu_3^{BF_3}$ region of the spectrum, recorded at 104 K, of a solution containing approximately 8.2×10^{-3} M COF_2 and 3.4×10^{-4} M BF_3, is compared with the monomer spectra. For both isotopes, in the mixed solution a broad, new band is observed on the low frequency side of the monomer absorption. In the complex, the degeneracy of $\nu_3^{BF_3}$ is lifted. For the anticipated complex **I**, the *ab initio* calculations predict a splitting of $\nu_3^{BF_3}$ into a high frequency component, red shifted by less than 3 cm^{-1}, and a low frequency component, shifted by nearly 14 cm^{-1}. Hence, doublets with a frequency splitting of some 11 cm^{-1} are expected. In the spectra, however, single maxima are observed, shifted by some 6 cm^{-1} from the monomer band. When the bands due to $COF_2 \cdot BF_3$ in Figure 6 are isolated by subtracting the monomer BF_3 contribution, their contours are found to substantially tail toward low frequency. The merging of nondegenerate bands into single, broad, asymmetric contours suggests they contain an important number of transitions, many of which start from states in which the asymmetry of the equilibrium structure is averaged out. Hence, the observed contours support the predicted nearly free internal rotation and large amplitude motions in the complex.

A new weak band is detected at 867.0 cm^{-1} in the spectra of solutions containing relatively high concentrations of the complex. As before[31,32] we assign this band to $\nu_1^{BF_3}$ which, due to symmetry lowering, becomes active in the complex.

The stoichiometry of the complex was determined as described previously.[31,39] In this analysis, the intensity of a complex band I_C is plotted, for various integer values of x and y, against $(I_{COF_2})^x \times (I_{BF_3})^y$, in which I_{COF_2} and I_{BF_3} are monomer band intensities. For the present case, mixed solutions were investigated at 110.4 K , in which the COF_2 concentrations were varied between 0.4×10^{-4} and 1.9×10^{-4} M, and that of BF_3 between 4.0×10^{-3} and 2.7×10^{-2} M. Intensities I_C and I_{COF_2} were obtained from a least squares band fitting of the $\nu_4^{COF_2}$ region. For I_{BF_3} the intensity of $\nu_1^{BF_3} + \nu_3^{BF_3}$ at 2375 cm^{-1} was used. Its corresponding complex mode appears red shifted by

(53) Dixon, R. N. *J. Chem. Phys.* **1959**, *31*, 258.
(54) Duncan, J. L.; Ellis, D.; Wright, I. J. *Mol. Phys.* **1971**, *20*, 673.
(55) McKean, D. C. *Spectrochim. Acta* **1973**, *29A*, 1559.

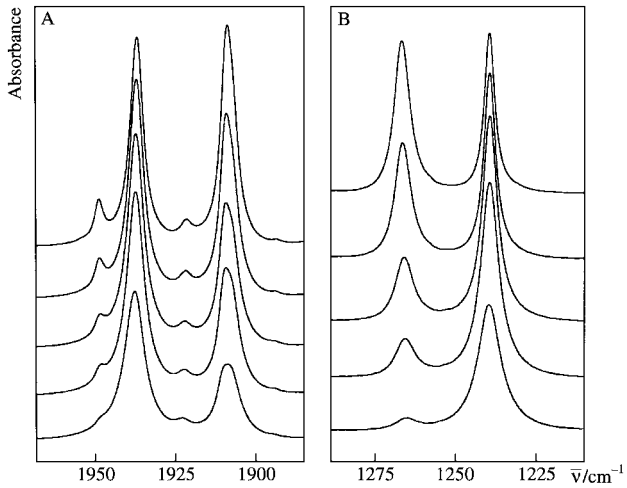

Figure 7. Temperature behavior of the spectra of COF_2/BF_3 mixtures dissolved in liquefied argon (A) and liquefied nitrogen (B). From top to bottom the temperature of the solutions increases form 106.4 to 125.4 K (A), and from 82.9 to 113.1 K (B).

11.4 cm^{-1}, which allows a reliable least squares band fitting to separate the monomer intensity. With these intensities, plots were prepared using 1 and 2 as values for x and y. Only for x and y equal to 1 a linear plot was obtained for concentrations of BF_3 smaller than 1.5×10^{-2} M. This proves that the observed complex has 1:1 stoichiometry. At higher concentrations of BF_3, deviations from linearity in the plot occur. Although no new bands are observed in the $\nu_4^{COF_2}$ region, it is believed that the deviation is caused by the measurable formation of a 1:2 complex $COF_2 \cdot (BF_3)_2$, its $\nu_4^{COF_2}$ being accidentally degenerate with the 1:1 band. The presence of a 1:2 complex is supported by the spectra in the $\nu_2^{COF_2}$ region, Figure 4b. It can be seen that at the highest concentrations a high frequency shoulder on the 1:1 band emerges near 977 cm^{-1}. The intensity ratio of this band to that of the 1:1 band at 973.2 cm^{-1} is concentration dependent, so it cannot be assigned to the 1:1 species. Therefore, we assign this band to the 1:2 complex.

The complexation enthalpy $\Delta H°$ was determined from a temperature study, using the van't Hoff isochore. From the latter can be shown that when the absorption coefficients are independent, or only weakly dependent, on temperature, $\ln[I_C/I_{COF_2} \times I_{BF_3}]$ is linearly related to $1/T$, and that the slope of this linear relationship equals $-(\Delta H° + b)/R$, in which R is the ideal gas constant and b is a correction for the thermal expansion of the solution.[56]

For the temperature studies in LAr and LN_2, a relatively low concentration of BF_3 was used, $\sim 8 \times 10^{-3}$ M, to minimize the fraction of 1:2 complexes. The LAr solutions were studied between 102 and 126 K, the LN_2 solutions between 81 and 113 K. The influence of temperature on the spectra is illustrated, using the ν_1 and ν_4 regions of COF_2, in Figure 7. For I_{BF_3} the integrated intensities of the bands at 2325 and 2375 cm^{-1} were used. The I_C and $ICOF_2$ were taken from fittings of the ν_1, ν_2, ν_4, and ν_6 regions of COF_2. For the ν_1 region the monomer and complex bands were first separated by the same subtraction techniques as used for Figure 5. van't Hoff plots were constructed using all possible combinations of I_C, I_{COF_2}, and I_{BF_3}. As an example, the plots using the 2375 cm^{-1} BF_3 band and the $\nu_2^{COF_2}$ bands are given in Figure 8. For each solvent, the different values for $\Delta H°$, calculated using published values of b,[56] fall within a narrow interval, showing that the assumption

(56) Van der Veken, B. J. *J. Phys. Chem.* **1996**, *100*, 17436.

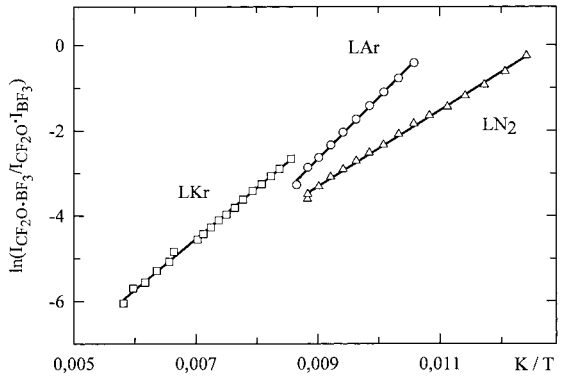

Figure 8. van't Hoff plots for $COF_2 \cdot BF_3$ dissolved in liquefied argon, krypton, and nitrogen.

of constant absorption coefficients is valid. The average $\Delta H°$ was found to be $-11.8(3)$ kJ mol^{-1} in LAr and $-7.8(3)$ kJ mol^{-1} in LN_2.

The temperature study in LKr was made in the range between 117 and 172 K. To ensure sufficiently intense complex bands, the BF_3 concentration was increased to 3.5×10^{-2} M. As above, influences of the 1:2 complex were neglected. For I_C and I_{COF_2} and the $\nu_2^{COF_2}$ bands were used. For I_{BF_3}, to avoid errors with detector saturation, the less intense absorption bands at 2983 and 2794 cm^{-1} were chosen. These bands are slightly asymmetric, and their intensities were measured by numerical integration. The van't Hoff plot for LKr shown in Figure 8 was derived using the 2983 cm^{-1} band. For reasons discussed below, the vertical axis for the LKr data in Figure 8 was shifted with respect to those for the LAr and LN_2 data. The average $\Delta H°$ obtained is $-10.6(3)$ kJ mol^{-1}.

Discussion

An important aspect is the type of complex that is observed in the cryosolutions. Comparison of the observed complexation shifts, Table 3, with the calculated ones, Table 2, shows that for $\nu_2^{COF_2}$ to $\nu_6^{COF_2}$ the observed shifts are in the direction predicted for isomer **I**. As the shifts in Table 2 were calculated in the harmonic approximation, for $\nu_1^{COF_2}$ they must be compared with the unperturbed shift given in Table 4. It is clear that also for this mode the observed direction is as predicted for isomer **I**. In contrast, the shifts predicted for **IIa** and **IIb**, with two minor exceptions, systematically are in a direction opposite to observation. Moreover, the quantitative agreement of the observed shifts with those for isomers **IIa** and **IIb** is very poor, while that for isomer **I** is excellent. For BF_3 the shifts for **IIa** and **IIb** are not in opposite direction of those for **I**, but comparison shows that the quantitative agreement for isomer **I** is much better than that for isomers **II**. Therefore, it may be concluded that the complex observed in this study has the structure of isomer **I**, in which the boron atom is coordinated to the oxygen atom. Careful inspection of the spectra in the regions where transitions due to isomers **IIa** and **IIb** are predicted gave no evidence for the presence of even the weakest transition. Thus, in agreement with the *ab initio* predictions, the complexation energies of **IIa** and **IIb** must be much smaller than that of isomer **I**. As to the 1:2 complex, it is clear from the discussion of the spectra that only one band of this species has been identified. Therefore, its structure remains a matter of speculation. As we have found no evidence of a 1:1 complex of type **II**, however, we prefer the structure in which both BF_3 molecules are attached to the oxygen atom, one on each side of the C═O axis.

The application of the intensity method[53−55] to the Fermi doublet, discussed above, also yields the Fermi resonance constant K_{122}. For monomer COF_2 this constant has been determined to be 27.6 cm^{-1} in argon matrices[25,36] by two different methods, and to be 27.5 cm^{-1} in LAr.[49] The result obtained here is 27.3 cm^{-1}, while for the complex the value of 29.6 cm^{-1} was found. The latter can be compared with the 28.0 cm^{-1} for $COF_2 \cdot Cl_2$ measured in an argon matrix.[36] Thus, at first sight the obtained data suggest that the Fermi resonance constant is affected by the complexation. However, it should be reminded that the intensity method[53−55] assumes that the IR intensity of the "unperturbed" $2\nu_2^{COF_2}$ mode, $I_{2\nu_2}^{unpert}$, is zero. The influence of neglecting the overtone intensity was investigated for both COF_2 and $COF_2 \cdot BF_3$ by evaluating K_{122} assuming a value of $I_{2\nu_2}^{unpert}$ as low as 0.1 km mol^{-1}. It is found that this changes K_{122} for the monomer by 0.3 cm^{-1} and for the complex by 0.8 cm^{-1}. Typically, a fundamental is 100 times more intense than its first overtone, so that from the DFT data $I_{2\nu_2}^{unpert}$ can be estimated to be 0.7 km mol^{-1}. With this value for $I_{2\nu_2}^{unpert}$, K_{122} for the monomer changes by 0.7 cm^{-1} and for the complex by 2.0 cm^{-1}. Therefore, it seems reasonable to adopt as uncertainty on K_{122} a value not less than 2 cm^{-1}. Consequently, the statistical significance of the difference between the experimental values of K_{122} obtained for monomer and complex is questionable.

The above analysis of the Fermi doublet is based on the simplifying assumption that the resonance can be described by a single Fermi resonance constant K_{122} that couples ν_1 and $2\nu_2$. Within this model, K_{122} equals $(1/2)\phi_{122}$, with ϕ_{122} the coefficient of a cubic term in the expression of the molecular potential expressed in normal coordinates[57]

$$\frac{V}{hc} = \frac{1}{2}\sum_i \omega_i q_i^2 + \frac{1}{6}\sum_{ijk} \phi_{ijk} q_i q_j q_k \qquad (3)$$

where ω_i is the frequency of mode *i*. As DFT calculations have been shown to accurately predict cubic force fields,[58] for COF_2 and $COF_2 \cdot BF_3$ the Cartesian cubic force field was calculated at the B3LYP/6-311++G(d,p) level, using Gaussian94.[42] The resulting Cartesian force field was transformed to the normal coordinate space using the program Spectro.[59] These calculations result in a value of 28.0 cm^{-1} for K_{122} of COF_2 and 27.7 cm^{-1} for $COF_2 \cdot BF_3$. The agreement with the experimental values is excellent, and the slightly smaller value for the complex appears to bear out our above conclusion on the reality of the difference between our experimental values.

One final remark on the Fermi resonance has to be made. The cubic force field yields the substantial value of 25.2 cm^{-1} for ϕ_{145}. The sum of ν_4 and ν_5 equals 1814.6 cm^{-1}, which puts the combination level in the vicinity of ν_1. Although no obvious intensification of $\nu_4 + \nu_5$ is observed in the spectra, from the value of ϕ_{145} it must be suspected that the observed intensity of ν_1 is somewhat affected by resonance with $\nu_4 + \nu_5$. This must reflect on the experimental K_{122} values, which adds to the notion that the uncertainty on K_{122} adopted above must be regarded as a lower limit.

The complexation enthalpy in LN_2 differs by 4.0(4) kJ mol^{-1} from that in LAr. This must be attributed[60] to differences in the behavior of BF_3 in the different solvents. Monte Carlo simulations[60] suggest that in LN_2 the BF_3 molecules are virtually completely complexed to a 1:2 species, $N_2 \cdot BF_3 \cdot N_2$, while for LAr no such complexes are formed. Thus, in LN_2 the complexation with carbonyl fluoride requires the breaking of a van der Waals bond between the boron atom and a nitrogen molecule. As a consequence, and neglecting all other effects, the difference in $\Delta H°$ between solutions in LN_2 and LAr must be equal to the complexation enthalpy for $BF_3 \cdot N_2$. The difference observed in this study indeed compares favorably with the complexation enthalpy of −4.8(3) kJ mol^{-1} derived in LAr for $BF_3 \cdot N_2$.[60]

The complexation enthalpies obtained for solutions in LAr and LKr can be transformed into a gas phase value by correcting for solvent effects. The latter can be subdivided into contributions due to (i) the cavity formation, (ii) dispersive, and (iii) electrostatic interactions.[61] As previously,[31,32,39,62] we neglect the contributions from the cavity formation and dispersive interactions, assuming the electrostatic contribution to be dominant.

To account for the electrostatic effect, Self-Consistent Isodensity Polarizable Continuum Model (SCIPCM) calculations[63] were performed at the B3LYP/6-311++G(d,p) level. The solute-solvent interaction free enthalpies, ΔG_{stab}, obtained from these calculations are collected in Table 5. They were transformed into stabilization enthalpies ΔH_{stab}, using the equation:

$$\frac{d(\Delta G_{stab}/T)}{dT^{-1}} = \Delta H_{stab} \qquad (4)$$

Since SCIPCM is based on the Onsager reaction field model,[64] the calculated stabilization free enthalpies are linearly related to the Kirkwood function $\chi = (\kappa - 1)/(2\kappa + 1)$, where κ is the relative permitivity of the medium. Assuming, that in such a relation only χ is temperature dependent, it can be shown that

$$\Delta H_{stab} = \Delta G_{stab}\left(1 + \frac{1}{T \cdot \chi} \cdot \frac{d\chi}{dT^{-1}}\right) \qquad (5)$$

For each solvent the values *T*, χ, and $(d\chi/dT^{-1})$ should be taken at the midpoint of the temperature interval under investigation. For LAr and LKr, the χ and $(d\chi/dT^{-1})$ values are either documented or can be calculated from the available data.[65] From these, and taking the midpoint temperatures for LAr and LKr to be 110 and 160 K, respectively, the coefficients of ΔG_{stab}, in (5) are found to be 1.51 (LAr) and 1.46 (LKr).

From the above values, and from the data in Table 5, the enthalpy destabilization of isomer **I** in LAr is found to be 1.5 kJ mol^{-1}, while for the LKr the value is 1.8 kJ mol^{-1}. Combining these with the $\Delta H°$ in solution, the vapor phase complexation enthalpy $\Delta H°_{gas}$ is calculated to be −13.3(3) and −12.4(3) kJ mol^{-1}, starting from the LAr and LKr results,

(57) Martin, M. L. J. *Accurate ab initio Calculation of Anharmonic Force Fields and Spectroscopic Constants of Small Polyatomic Molecules*; University of Antwerp: Antwerp, 1994; p 7.
(58) Dressler, S.; Thiel, W. *Chem. Phys. Lett.* **1997**, *237*, 71.
(59) Gaw, J. F.; Willetts, A.; Green, W. H.; Handy, N. C. In *Advances in Molecular Vibrations and Collision Dynamics*; Bowman, J. M., Ed.; JAI Press: Greenwich, CT, 1990.
(60) Herrebout, W. A.; Van der Veken, B. J. Manuscript in preparation.
(61) Samoshin, V. V.; Zefirov, N. S. *Zh. Vses. Khim. Ova. (USSR)* **1984**, *29*, 521.
(62) Herrebout, W. A.; Everaert, G. P.; Van der Veken, B. J.; Bulanin, M. O. *J. Chem. Phys.* **1997**, *107*, 8886.
(63) Foresman, J. B.; Keith, T. A.; Wiberg, K. B.; Snoonian, J.; Frish, M. J. *J. Phys. Chem.* **1996**, *100*, 16098.
(64) Simkin, B. Ya.; Sheikhet, I. I. *Quantum Chemical and Statistical Theory of Solutions: a Computational Approach*; Ellis Howard Ltd: London, 1995.
(65) Bulanin, M. O.; Zelikina, G. Ya. In *Molecular Cryospectroscopy*; Clark, R. J. H.; Hester, R. E., Eds.; Wiley: Chichester, 1995; p 22.

Table 5. SCRF=SCIPCM Electrostatic Stabilization Free Energies (kJ mol^{-1}) for Carbonyl Fluoride, Boron Trifluoride, and Various 1:1 Complexes[a]

molecule/adduct	solvent	
	LAr	LKr
COF_2	2.065	2.499
BF_3	2.537	3.077
I	3.592	4.326
IIa	3.791	4.597
IIb	3.733	4.529

[a] All values were calculated on the B3LYP/6-311++G(d,p) level.

respectively. The uncertainties quoted are those of the experimental values. As the solvent corrections are approximate, these uncertainties presumably are somewhat underestimated. The $\Delta H°$ for LAr and LKr in solutions were measured at different temperatures, so that the gas phase values derived from them correspond to different temperatures. Thus, it must be expected that the difference between the gas phase values is due to the different thermal contributions to the $\Delta H°$.

In a next step the $\Delta H°_{gas}$ were transformed into complexation energies $\Delta_c E$, using equations of standard statistical thermodynamics.[66] For all species the zero-point vibrational energies were calculated using the *ab initio* frequencies. Thermal contributions were evaluated at the midpoints of the temperature intervals, 104 K for the LAr result and 133 K for the LKr result. Translational and rotational thermal contributions were obtained in the classical limit, and vibrational thermal contributions were evaluated in the harmonic approximation,[66] using the same frequencies as for the zero-point corrections. All this results in the following complexation energies

$$\Delta_c E(\mathrm{LAr}) = \Delta H°_{gas}(\mathrm{LAr}) - 2.02\ \mathrm{kJ\ mol^{-1}} = -15.3(6)\ \mathrm{kJ\ mol^{-1}} \quad (6)$$

$$\Delta_c E(\mathrm{LKr}) = \Delta H°_{gas}(\mathrm{LKr}) - 2.43\ \mathrm{kJ\ mol^{-1}} = -14.8(6)\ \mathrm{kJ\ mol^{-1}} \quad (7)$$

The uncertainties are, somewhat arbitrarily, chosen to be twice the value for $\Delta H°$ to account for the approximations made in transforming $\Delta H°$ to $\Delta_c E$. If the applied corrections are physically reasonable, complexation energies derived from enthalpies measured in different solvents and different temperature intervals should be identical. It can be seen that this is the case, even within the smaller experimental error limits. Therefore, we propose to take the average value, -15.0 ± 0.6 kJ mol^{-1}, as the experimental complexation energy of the 1:1 complex.

The B3LYP/6-311++G(d,p) complexation energy for **I** was calculated above to be -9.87 kJ mol^{-1}. This value is significantly smaller than the experimental one. Correction for Basis Set Superposition Error (BSSE)[67] by the counterpoise method of Boys and Bernardi[68] results in -6.98 kJ mol^{-1}, which is even further away from the experimental value. This shows that at the B3LYP/6-311++G(d,p) level the calculations seriously underestimate the stability of the 1:1 complex. This, most probably, is due to the fact that the present DFT calculations do not include the attractive dispersion interactions between molecules.[69−72] The problem is well known, and recently a procedure has been devised[73,74] to improve the situation. The procedure involves a DFT geometry optimization, followed by a single-point post-Hartree−Fock calculation. Starting from the B3LYP/6-311++G(d,p) geometries for the monomers and for isomer **I**, an MP2 single point calculation was made using Dunning's augmented correlation consistent polarized valence triple-ζ basis set, also noted as aug-cc-pVTZ.[75−77] The resulting complexation energies, before and after correcting for BSSE, are -22.1 and -12.4 kJ mol^{-1}. The uncorrected energy overestimates the experimental one. In contrast, the corrected complexation energy is somewhat smaller than the experimental value. This is consistent with the predicted overcorrection of the BSSE when using the counterpoise method at the correlated level.[78,79] Altogether, it is clear that this procedure results in a better value for the complexation energy.

For the dilute solutions used in this study, Beer's law can be used to transform the van't Hoff equation into

$$\ln \frac{I_C}{I_{COF_2} \times I_{BF_3}} + \ln \frac{A_{COF_2} \times A_{BF_3}}{A_C} = -\frac{\Delta H°}{RT} + \frac{\Delta S°}{R} \quad (8)$$

where the A_i are the integral absorption coefficients and $\Delta S°$ is the complexation entropy. Since the dielectric constants of the solutions used here are relatively small and do not vary significantly from one solvent to another,[65] it is reasonable to assume that the integral absorption coefficients, A_i, determined at a certain temperature, do not depend on the solvent. Then, the term $\ln[A_{COF_2} \times A_{BF_3}/A_C]$ is taken to have the same value for all solvents used. It was shown above that the $\Delta H°$ for $COF_2 \cdot BF_3$ changes by 4.0 kJ mol^{-1} from LAr to LN_2. If we assume that the complexation entropy is the same in all solvents, the above equation shows that at 100 K the distance between the regression lines for LAr and LN_2 in Figure 8 should be -4.7 units of the vertical scale. However, it can be seen that this distance is substantially less. Thus, $\Delta S°$ cannot be the same in the two solvents. The absorption coefficients A_i have not been measured, and their presence in eq 8 prevents $\Delta S°$ to be calculated. However, the equation can be used to evaluate the change in $\Delta S°$ between two solvents:

$$\Delta\Delta S° = (\Delta S°)_{solvent} - (\Delta S°)_{solvent2} \quad (9)$$

The $\Delta\Delta S°$ between solutions in LAr and LN_2 was determined using the regression lines for the van't Hoff plot constructed from the 2375 cm^{-1} (I_{BF_3}) and the $\nu_1^{COF_2}$, the $\nu_2^{COF_2}$ and $\nu_4^{COF_2}$ doublets (I_C, I_{COF_3}). The values obtained are 26(4), 29(4), and 21(4) kJ mol^{-1} K^{-1}, respectively. As it is unlikely that solvent influences alter A_i of different vibrations to the same extent, the similarity of these $\Delta\Delta S°$ supports the assumption of solvent

(66) Knox, J. H. *Molecular Thermodynamics. An Introduction to Statistical Thermodynamics for Chemists*; Wiley-Interscience: London, 1971.
(67) Van Duijneveldt, F. B. In *Molecular Interactions: from Van der Waals to Strongly Bound Systems*; Scheiner, S., Ed.; Wiley: Chichester, 1997; p 81.
(68) Boys, S. B.; Bernardi, F. *Mol. Phys.* **1970**, *19*, 553.
(69) Okhissi, A.; Alikhani, M. E.; Bouteiller, Y. *J. Mol. Struct.* **1997**, *416*, 1.
(70) Ruiz, E.; Salahub, D. R.; Vela, A. *J. Am. Chem. Soc.* **1995**, *117*, 1141.
(71) Ruiz, E.; Salahub, D. R.; Vela, A. *J. Phys. Chem.* **1996**, *100*, 12265.
(72) Del Bene, J. E.; Deison, W. B.; Szczepaniak, K. *J. Phys. Chem.* **1995**, *99*, 10705.
(73) Del Bene J. E.; Shavitt, I. A. in *Molecular Interactions: from Van der Waals to Strongly Bound Systems*; Scheiner, S., Ed.; Wiley: Chichester, 1997; p 157.
(74) Herrebout, W. A.; Van der Veken, B. J. Unpublished results.
(75) Dunning, T. H., Jr. *J. Chem. Phys.* **1989**, *90*, 1007.
(76) Kendall, R. A.; Dunning, T. H., Jr.; Harisson, R. J. *J. Chem. Phys.* **1992**, *96*, 6796.
(77) Woon, D. E.; Dunning, T. H., Jr. *J. Chem. Phys.* **1993**, *98*, 1358.
(78) Rayon, Y. M.; Sordo, J. A. *J. Phys. Chem. A* **1997**, *101*, 7414.
(79) Suares, D.; Sordo, T. L. *J. Phys. Chem.* **1996**, *100*, 13462.

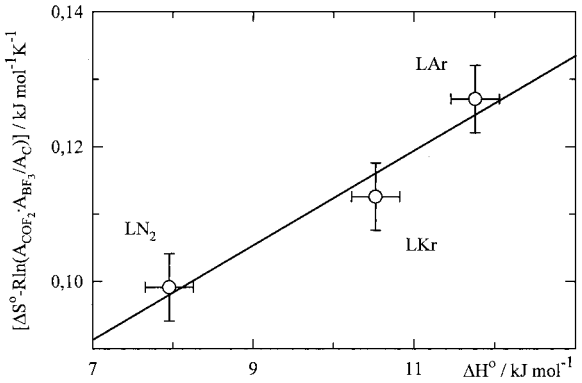

Figure 9. Correlation between $\Delta S°$ and $\Delta H°$ for the complexation of COF_2 with BF_3 in different solvents.

independent absorption coefficients. It is clear from relation (8) that for a comparison of results from different solvents, the same A_i must be used. The van't Hoff plots for LKr, however, were determined using the 2983 and 2794 cm^{-1} bands of BF_3, while for LAr and LN_2 the results in eq 8 are based on the bands at 2375 and 2983 cm^{-1}. Therefore, the experimental I_{BF_3} were rescaled with the ratio of either the 2375 and 2982 cm^{-1} bands or the 2375 and 2794 cm^{-1} bands. These ratios were measured for more dilute solutions of BF_3 in LKr and were found to be 2.3(1) and 5.2(1), respectively. The LKr data shown in Figure 8 are based on such rescaled intensities.

Using the regression lines for the van't Hoff plots constructed from the $\nu_2^{COF_2}$ doublets, eq 8 was applied to calculate the $[\Delta S° - R \ln(A_{COF_2} \times A_{BF_3}/A_C)]$ values for the different solvents. In Figure 9 they have been plotted against the corresponding values of $\Delta H°$.

Within the error limits, Figure 9 shows a linear correlation with a positive slope, equal to $7.0(3.5) \times 10^{-3}$ K^{-1}. Since the terms of eq 8 containing $\Delta H°$ and $\Delta S°$ have the opposite signs, the positive slope indicates a partial compensation of the enthalpy contribution to the equilibrium constant by the entropy one. Correlations between $\Delta H°$ and $\Delta S°$, known as the compensation effect, were observed in various fields of physical chemistry, including thermodynamics of solvation,[80,81] hydrogen bonding,[82,83] and conformational analysis.[84−86] Similar correlations but between the kinetic values of activation enthalpy and entropy were also found.[87] To our knowledge, this work gives the first evidence of the compensation effect for the thermodynamics of van der Waals complexes.

The origin of the compensation effect lies in the fact that stronger interactions usually produce more ordered molecular systems, or, the larger is the absolute value of $\Delta H°$, the more negative is the value of $\Delta S°$. Since the systems under study include both solute and solvent molecules, a detailed analysis of the contributions to the effect is hardly possible at the present stage. Finally, it may be noted that the slope obtained for the $COF_2 \cdot BF_3$ complex is much larger than the mean values reported for various conformational equilibria,[84−86] 1.3×10^{-3} K^{-1}, and H-bonded complexes complexes,[83] 2.5×10^{-3} K^{-1}.

Acknowledgment. W.A.H. thanks the Fund for Scientific Research (FWO, Belgium) for an appointment as Postdoctoral Fellow. The FWO is also thanked for financial help toward the spectroscopic equipment used in this study. Support by the Flemish Community, through the Special Research Fund (BOF) is gratefully acknowledged. The authors are grateful to C. De Meyer for his kind help in transforming the cubic force field from Cartesian to normal coordinates and to Dr. M. D. Borisover for fruitful discussions.

JA980874+

(80) Solomonov, B. N.; Gorbachuk, V. V.; Konovalov, A. I. *Zh. Obsch. Khim. (USSR)* **1982**, *52*, 2688.
(81) Abraham, M. H., Whiting, G. S., Fuchs, R.; Chambers, E. J.; *J. Chem. Soc., Perkin Trans.* 2 **1990**, 291.
(82) Pimentel, G. C.; McClellan, A. L. *The Hydrogen Bond*; Freeman: San Francisco, 1960.
(83) Goldshtein, I. P.; Guryanova, E. N.; Shcherbakova, E. S. *Zh. Obsch. Khim. (USSR)* **1970**, *40*, 183.
(84) Fishman, A. I.; Stolov, A. A.; Remizov, A. B. *Spectrochim. Acta*, **1993**, *49A*, 1435.
(85) Stolov, A. A.; Remizov, A. B. *Spectrochim. Acta* **1995**, *51A*, 1919.
(86) Stolov, A. A.; Kohan, N. V.; Remizov, A. B. *Vibrational Spectrosc.* **1997**, *14*, 35.
(87) House, J. E. *Principles of Chemical Kinetics*; Wm. C. Brown Publishers: Dubuque, 1997.